
Orientation definition of anisotropy is important to finite element simulation of bone material properties

Release 2.11

Haisheng Yang^{1,2}, Tongtong Guo¹ and Xin Ma^{2,3}

May 21, 2008

¹Harbin Institute of Technology Shenzhen Graduate School

²Shenzhen Institute of Advanced Technology, Chinese Academy of Sciences

³Harbin Institute of Technology

Abstract

The assignment of bone material properties to finite element model is a fundamental step in finite element analysis and has great influence on analysis results. Most work done in this area has adopted isotropic assignment strategy as its simplicity. However, bone material is widely recognized as being anisotropic rather than isotropic. Therefore, this work is aimed to simulate the inhomogeneity and anisotropy of femur by assigning each element of the mesh model the material properties with a numerical integration method and properly defining the principal material orientation, and then compare the biomechanical analysis results of isotropic model with that of anisotropic model under six different loading conditions. Based on the analysis results of the equivalent Von Mises stress and the nodal displacement, four different regions of interest are chosen to achieve this comparison. The results show that significant differences between the two material property assignments exist in the regions where anisotropic material property is sensitive to orientation definition. Thus, orientation definition is important to finite element simulation of bone material properties.

Contents

1	Introduction	2
2	Materials and methods	3
2.1	CT data	3
2.2	Finite element mesh	3
2.3	The procedure of material property assignment	4
2.3.1	Calculation of the average CT number	4
2.3.2	Calibration of the CT dataset	4
2.3.3	Calculation of the elastic constants	4
2.4	The definition of material orientation	5

2.5	Loading conditions	5
2.6	Comparison of isotropic and orthotropic material property assignments	6
3	Results	7
3.1	Inhomogeneous distribution of material properties	7
3.2	The definition of principal material orientation (orthotropic FE-simulation)	8
3.3	Differences between isotropic and orthotropic material models	8
4	Discussion	9

1 Introduction

Finite element (FE) analysis, as a non-invasive method, has been widely used in academic research and clinical applications, such as the theory of bone remodeling [1], the design of prosthesis [2] and the evaluation of fracture risk [3]. Accurate simulation of bone biomechanical behavior depends on not only the accurate model obtained via three-dimensional reconstruction, but also the realistic material properties that consist with different aspects' bone density and anatomical structure.

In early period, the methods used to get bone geometry and mechanical properties were inaccurate and sometimes highly invasive and destructive. It is well known that CT images can provide fairly accurate quantitative information on bone geometry based on high contrast between the bone tissue and the soft tissue around [4]. Moreover, it has been demonstrated that CT numbers are almost linearly correlated with apparent density of biologic tissues [5]. Good experimental relationships have been established between density and mechanical properties of bone tissues [6].

The CT data can be regarded as a three-dimensional scalar field (related to the tissue density) sampled over a regular grid. Once the finite element mesh is generated starting from the same CT data, the mesh and the density distribution are perfectly registered in space. The only problem is how to properly map the density into the finite element mesh. Many approaches were proposed in literature to perform this task [7-10]. However, these algorithms only simulated the inhomogeneity of bone material, and the isotropic material property assignment was adopted without considering the material orientation of bone tissue. Since the bone material is anisotropic [11, 15, 16], the isotropic FE simulation of bone material property cannot reflect the actual structure and mechanical behavior of bone.

In recent studies, more attentions were paid to the orthotropic material property assignment and the comparison between isotropic and orthotropic methods. Peng et al [12] compared isotropic material property assignment with orthotropic assignment on femoral finite element models and demonstrated that the differences were small and bone is weak orthotropic material. Nevertheless, the global coordinate system was defined as the orthotropic orientation over the whole femoral model. This definition can not respect the real anatomical locations in femur, especially in femoral neck. The results, therefore, were distorted. Baca et al [13] overcame abovementioned shortcomings by manually defining orthotropic orientation based on real anatomical structure that was obtained following a grinding protocol. However, too much manual work needs to be done and the investigator must be quite familiar with anatomical

structure of femur. Besides, this method can only be applicable to cadaveric bone. What's more, the data used for comparison are too little to doubtless support the conclusion. Unfortunately, both studies mistook the unit of shear modulus (GP) for unit (MP) when they quoted the formula of density-modulus relationship in [15] ($G_{12\max} = 5.71\text{ GP}$, $G_{23\max} = 7.11\text{ GP}$, $G_{31\max} = 6.58\text{ GP}$). Moreover, the force (8kN) applied to femoral head was almost ten times to the weight of a normal person. This force may destroy the bone structure or produce abnormal stress and displacement.

This work is aimed to simulate the inhomogeneity and anisotropy of femur by properly defining the principal material orientation automatically, and investigate the differences between isotropic and orthotropic material property assignments through correctly defining the material orientation and exactly using the parameters.

2 Materials and methods

2.1 CT data

The CT dataset of a man's femur is obtained from the public database which is created by VAKHUM project (<http://www.ulb.ac.be/project/vakhum/index.html>). The use of the data is free for academic purposes. The CT data are in standard DICOM formats. The slice thickness is 1mm in the epiphysis and 3mm in the diaphysis.

2.2 Finite element mesh

The finite element mesh of a right femur (Figure 1) generated from the corresponding CT dataset above is also obtained from the VAKHUM project. It is in a Patran Neutral file format. The mesh is made of linear hexahedral elements and is generated using the HEXAR (Cray Research, USA) automatic mesh generator that implements a grid-based meshing algorithm. The model mesh is spatially registered with the CT dataset. The complete finite element mesh consisted of 9,294 nodes and 7,934 elements.

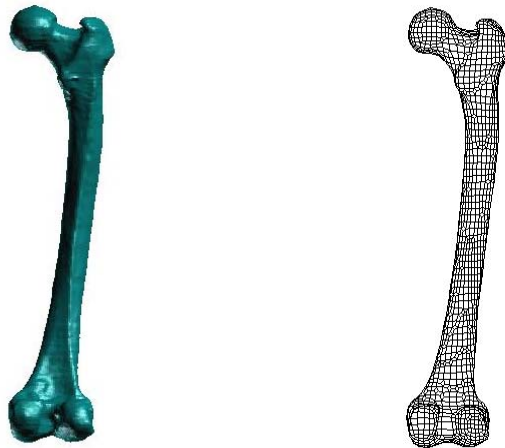


Figure 1 (a) The geometrical model of femur. (b) The finite element mesh of femur.

2.3 The procedure of material property assignment

2.3.1 Calculation of the average CT number

For each element of the mesh, an average HU value is calculated with a numerical integration as follows:

$$\begin{aligned}\overline{HU}_n &= \frac{\int_{V_n} HU(x, y, z) dV}{\int_{V_n} dV} \\ &= \frac{\int_{V'_n} HU(r, s, t) \det J(r, s, t) dV'}{V_n}\end{aligned}\quad (1)$$

where V_n indicates the volume of the element n , (x, y, z) are the coordinates in the CT reference system, (r, s, t) are the local coordinates in the element reference system, and J represents the Jacobian of the transformation. The integrals in Equation 1 are evaluated numerically, and the order of the numerical integration can be chosen by us. The value of $HU(x, y, z)$ in a generic point of the CT domain is determined by a tri-linear interpolation between the eight adjacent grid points' values.

2.3.2 Calibration of the CT dataset

It has been demonstrated that the relationship between CT number and apparent density is linear. The calibration equation is then:

$$\overline{\rho}_n = \alpha + \beta \overline{HU}_n \quad (2)$$

where $\overline{\rho}_n$ is the average density assigned to the element n of the mesh, \overline{HU}_n is the average CT number and α , β are the coefficients provided by calibration.

Generally, a calibration phantom [14] was used to obtain the parameters of the linear regression. In this paper, referenced values are selected for approximate calibration from [7]: Radiographic and apparent density of water (0 HU, 1 g/cm³); Average radiographic density in the cortical region and the apparent density value for cortical bone (1840 HU, 1.73 g/cm³).

2.3.3 Calculation of the elastic constants

Large number of experiments shows that the bone material properties can be expressed as function of apparent density, and various experimental relationships between elastic modulus and apparent density can be found in the literature. In the case of isotropic material property:

- Cortical bone:

$$E = 2065 \rho^{3.09}, \nu = 0.3 \quad (3)$$

- Cancellous bone:

$$E = 1094\rho^{1.64}, \nu = 0.3 \quad (4)$$

where E is the average Young's modulus assigned to the element n of the mesh, ρ is its apparent density and ν is the Poisson ratio.

In the case of orthotropic material property:

- Cortical bone:

$$E_1 = E_2 = 2314\rho^{1.57}, E_3 = 2065\rho^{3.09}$$

$$\nu_{12} = 0.58, \nu_{13} = \nu_{23} = 0.32$$

$$G_{12} = E_1 / 2(1 + \nu_{12}), G_{13} = G_{23} = 3.3 \quad (5)$$

- Cancellous bone:

$$E_1 = E_2 = 1157\rho^{1.78}, E_3 = 1094\rho^{1.64}$$

$$\nu_{12} = 0.58, \nu_{13} = \nu_{23} = 0.32$$

$$G_{12} = E_1 / 2(1 + \nu_{12}), G_{13} = G_{23} = 0.11 \quad (6)$$

where E is the Young's modulus (MPa), G the shear modulus (GPa), ν the Poisson's ratio. The coordinate systems of these parameters are defined in next step. In order to get a limited number of material card, a ΔE_3 threshold is chosen in the program. In this work, $\Delta E_3 = 50$ MP.

2.4 The definition of material orientation

As we know, bone structure is customarily recognized as confirming to 'wolff's law' which is essentially the observation that bone changes its external shape and internal architecture in response to stresses acting on it. Thus, the structure of bone (or material orientation) strongly coincides with the principal stress track. Since bone tissue is recognized as orthotropic material, the determination of principal material orientation based on real anatomical bone structure is essential to the real simulation of bone material properties. According to the cortical bone structure in femoral stem and cancellous bone structure in femoral neck, the principal material orientation of cancellous bone is defined by the direction of the trabecular structures and the principal material orientation of cortical bone by the direction of the haversian system.

2.5 Loading conditions

After the generation of finite element models with bone material properties and orthotropic orientation, six loading conditions (Figure 2) are applied to the isotropic models and orthotropic models respectively:

- LC1. Neutral: femoral axis vertical.
- LC2. Maximum adduction: 24° in the frontal plane.
- LC3. Maximum abduction: 3° in the frontal plane.

- LC4. Maximum flexion: - 3° in the sagittall plane.
- LC5. Maximum extension: 18° in the sagittall plane.
- LC6. High stress in neck: 8° in the frontal plane.

The force (500N) is applied on femoral head based on the local reference coordinate system defined in [18] and the distal femur is fully constrained.

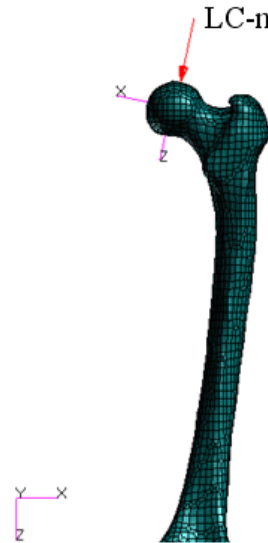


Figure 2 Boundary conditions and local reference coordinate system.

2.6 Comparison of isotropic and orthotropic material property assignments

The objective of this study is to investigate the differences between isotropic and orthotropic material property FE-simulation. Thus, two parameters are defined to show the differences. The first parameter ($\Delta\sigma$) represents the difference of equivalent Von Mises stress in the regions of interest (ROI) between isotropic and orthotropic models. The second parameter (Δu) represents the difference of nodal displacement in ROI:

$$\Delta\sigma^n = \left| \frac{\sigma_i^n - \sigma_o^n}{\sigma_o^n} \right| \quad (7)$$

$$\Delta u^n = \left| \frac{u_i^n - u_o^n}{u_o^n} \right| \quad (8)$$

where $\Delta\sigma^n$ is the difference of stress in ROI n ($n=1,2,3,4$), $\Delta\sigma_i^n$ and $\Delta\sigma_o^n$ represent the parameter $\Delta\sigma^n$ in case of the isotropic material property assignment and the orthotropic material property assignment. Δu^n is the difference of stress in ROI n ($n=1,2,3,4$), Δu_i^n and Δu_o^n represent the parameter Δu^n in case of the isotropic material property assignment and the orthotropic material property assignment.

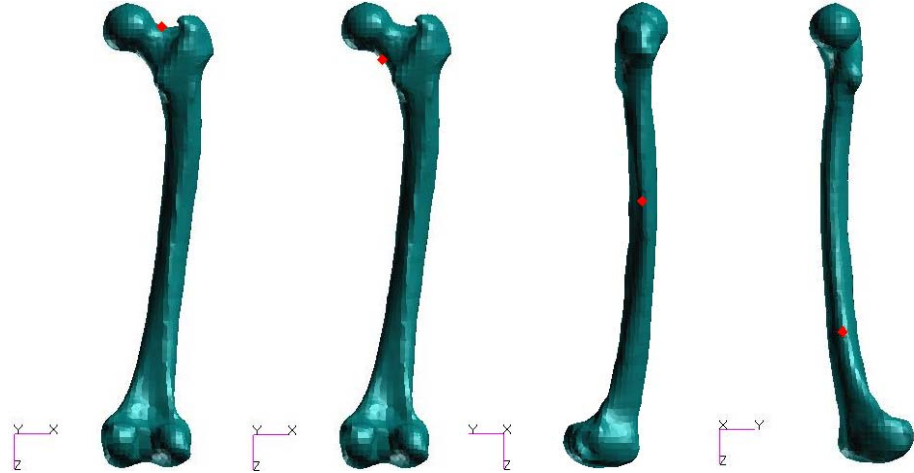


Figure 3 Four regions of interest: ROI1 in superior neck, ROI2 in inferior neck, ROI3 in diaphysis and ROI4 in distal femur.

In order to make the compared results more comprehensive, four different regions of interest (including femoral neck, diaphysis and distal femur) are chosen for comparison instead of only comparing the maximum value of Von Mises stress and nodal displacement (Figure 3).

3 Results

3.1 Inhomogeneous distribution of material properties

This material assignment procedure produces 165 different material definitions. The distribution of all kinds of material properties in femur are shown in Figure 4.

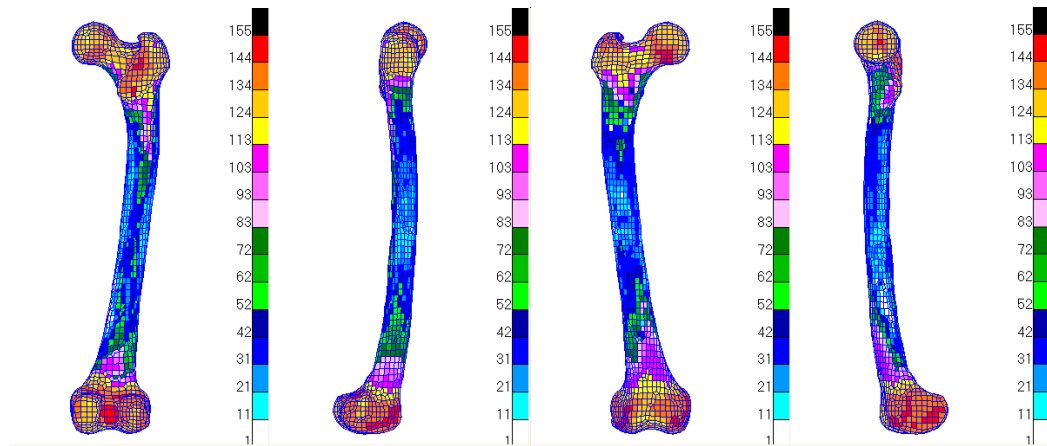


Figure 4 Right femur with different material properties mapped on it: posterior, lateral, anterior and medial views.

The maximum and minimum values for apparent density and elastic modulus are listed in Table 1. The maximum is corresponding to the material property 1 and the minimum to number 165 as a result of the definition in the program.

	Material properties		
	ρ	$E_1(E_2)$	E_3
Maximum	1.787	5755.799	12410.846
Minimum	0.686	591.512	1026.157

Table 1 Density and elastic modulus (The unit for density is g/cm³, and for elastic modulus is MP).

3.2 The definition of principal material orientation (orthotropic FE-simulation)

After separating the femoral neck and stem, different principal material orientations are automatically assigned to the two aspects. As is shown in Figure 5: In femoral neck, the principal axis is along the direction of neck which has an angle 120° to z axis; In femoral stem, the principal axis is along the direction of stem which has an approximate angle 12° to z axis. Besides, the other two transverse axes are defined perpendicular to the z axis.

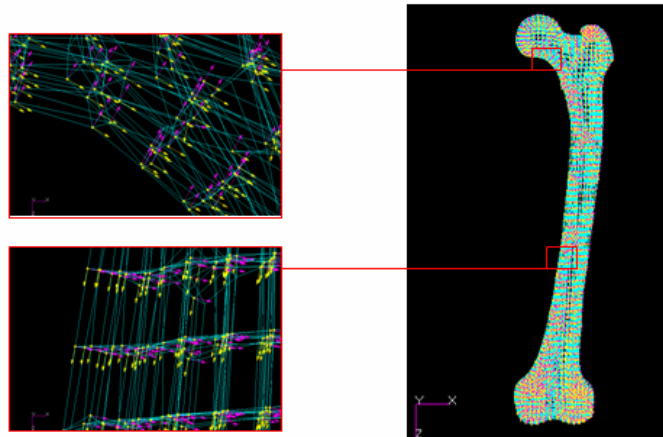


Figure 5 Orthotropic FE model with principal material orientation presented in vector form.

3.3 Differences between isotropic and orthotropic material models

Table 1 shows the relative differences of equivalent Von Mises stress $\Delta\sigma$ in four regions (ROI1-ROI4) under six loading conditions (LC1-LC6). Table 2 shows the relative differences of nodal displacement Δu . Under each loading condition, the change of data from ROI1 to ROI4 is quite similar. For equivalent Von Mises stress, two material property assignments show marked differences in ROI1: the values of $\Delta\sigma$ are from 16.63% to 18.17%. Significant differences still appear in ROI2: the values of

$\Delta\sigma$ are greater than 9.96% and the maximum reaches 11.67%. On the contrary, the differences of stress between two material property assignments are lower than 0.41% in ROI3 and 1.62% in ROI4.

For nodal displacement, the values of Δu are nearly 5% in ROI1, ROI2 and ROI3 under all the loading conditions except LC2 and LC5. The differences are larger than 8.67% in ROI4 and bigger values of Δu exist here under LC2 and LC5: 17.73% for LC2 and 15.77% for LC5.

Regions of interest	Loading conditions					
	LC1	LC2	LC3	LC4	LC5	LC6
ROI1	18.17	16.63	17.78	18.10	17.14	17.97
ROI2	11.09	9.99	11.63	11.67	11.16	9.96
ROI3	0.29	0.35	0.27	0.41	0.39	0.26
ROI4	0.91	1.62	1.01	1.21	0.57	1.35

Table 1 The relative differences of stress $\Delta\sigma$ in four regions of femur under six loading conditions (%).

Regions of interest	Loading conditions					
	LC1	LC2	LC3	LC4	LC5	LC6
ROI1	4.22	8.43	4.33	4.74	6.55	4.69
ROI2	4.25	9.33	4.41	4.95	7.03	4.90
ROI3	4.07	7.42	3.90	4.06	6.26	3.69
ROI4	8.67	17.73	9.29	11.27	15.77	11.59

Table 2 The relative differences of displacement Δu in four regions of femur under six loading conditions (%).

4 Discussion

The finite element method has been increasingly accepted as a useful tool to study the biomechanical behavior of bone structure. As we know, CT data can offer not only the accurate information on bone geometry but also the density information which has been demonstrated having relationship with bone material properties. Once the finite element mesh has been generated from CT data, how to assign the realistic material properties to finite elements becomes crucial for the FEA. Most work done in this domain only simulates the inhomogeneity and isotropy of bone as its simplicity. Bone, however, is widely recognized as anisotropic material and can be simplified to orthotropic material that has nine independent elastic constants and spatial orientation of the principal axes of orthotropy.

It has been demonstrated that the structure of femur is highly variable, especially to cancellous bone. Thus, a clear and exact definition of the principal axes of orthotropy is impossible. In this study, we only separate the femoral neck and stem. Then, the principal orientations of neck are defined on the basis of the direction of trabecular structure and the principal orientation of stem on the basis of the direction of harversian system. As the structure of femur (or material orientation) coincides with the track of principal stress, the orientation definition based on pass of stress is reasonable.

In order to roundly investigate the differences between the isotropic model and orthotropic model, equivalent Von Mises stresses and nodal displacements from four regions of femur are chosen to achieve this comparison. As shown in Table 1, significant differences appear in ROI1 and ROI2: the maximum of $\Delta\sigma$ reach 18.17% and 11.67% respectively. ROI1 and ROI2 located in femoral neck where the principal material orientations are defined according to the trabecular structure and have great differences with the global coordinate system. Consequently, it is considered that anisotropic material property is sensitive to orientation definition in these regions. The results indicate that large differences of stress just exist in these regions. The differences of stress are lower in ROI3 and ROI4 where the principal material orientation only has an angle 12° to z axis of the global coordinate.

For nodal displacement, the differences are lower in ROI1, ROI2 and ROI3 (about 5% for Δu). But, nodal displacements for two models show obvious differences in ROI4. According to the analysis results in both models, we find that there are fewer displacements in ROI4. This means significant differences between isotropic and orthotropic models may appear in these regions where absolute displacements are lower. Moreover, largest equivalent Von Mises stress is in the ROI4 where the differences are quite small. Therefore, incorrect results may be obtained if researchers compare the differences with maximum equivalent Von Mises stress and maximum nodal displacement.

In this study, six loading conditions are applied to the models aiming to investigate whether different loads have influence on compared results. As shown in Table 2, the values of Δu under LC2 and LC5 are obviously different from others. Thus, different loading conditions will lead to different comparison results. Besides, the loading conditions have different effects on stress and displacement.

With the comparison of isotropic and orthotropic material property assignments on femoral finite element models, significant differences exist in the regions where anisotropic material property is sensitive to orientation definition. Therefore, it is inaccurate to simplify orthotropy to isotropy during the procedure of material properties FE-simulation and orientation definition is important to the finite element simulation of material property.

How to simulate the real material properties of bone with finite element method is a problem all the while. Although since several years, some studies have been performed to generate anisotropy FE modeling of femur, these models can not reproduce exactly in vivo conditions. In our study, the principal material orientations are defined according to the macroscopical structure that consists with the stress pass. Thus, this method has reproducibility. Future work has to be done to validate the anisotropy model via experiment.

Reference

- [1] P.R. Fernandes, J. Folgado, C. Jacobs, V. Pellegrini. A contact model with ingrowth control for bone remodeling around cementless stems. *Journal of Biomechanics*, 35:167-176, 2002.

- [2] P. Kowalczyk. Design optimization of cementless femoral hip prostheses using finite element analysis. *Journal of Biomechanics*, 123:396-402, 2001.
- [3] J. H. Keyak. Improved prediction of proximal femoral fracture load using nonlinear finite element models. *Medical Engineering and Physics*, 23:165-173, 2001.
- [4] M. Viceconti, L. Bellingeri, L. Cristofolini, and A. Toni. A comparative study on different methods of automatic mesh generation of human femurs. *Medical Engineering and Physics*, 20:1-10, 1998.
- [5] J. Y. Rho, M. C. Hobatho, and R. B. Ashman. Relations of mechanical properties to density and CT numbers in human bone. *Medical Engineering and Physics*, 17:347-355, 1995.
- [6] D.C. Wirtz, N. Schifflers, T. Pandorf, K. Radermacher, D. Weichert, and R. Forst. Critical evaluation of known bone material properties to realize anisotropic FE-simulation of the proximal femur. *Journal of Biomechanics*, 33:1325-1330, 2000.
- [7] C. Zannoni, R. Mantovani, and M. Viceconti. Material properties assignment to finite element models of bone structures: a new method. *Medical Engineering and Physics*, 20:735-740, 1998.
- [8] F. Taddei, A. Pancanti, and M. Viceconti. An improved method for the automatic mapping of ct numbers onto finite element models. *Medical Engineering and Physics*, 26:61-69, 2004.
- [9] F. Taddei, E. Schileo, B. Helgason, L. Cristofolini, and M. Viceconti. The material mapping strategy influences the accuracy of CT-based finite element models of bones: an evaluation against experimental measurements. *Medical Engineering and Physics*, 29:973-979, 2007.
- [10] B. Helgason, F. Taddei, H. Palsson, E. Schileo, L. Cristofolini, M. Viceconti, and S. Brynjolfsson. A modified method for assigning material properties to FE models of bones. *Medical Engineering and Physics*, 30:444-453, 2007.
- [11] R. B. Ashman, S. C. Cowin, W. C. Van Buskirk, and J. C. Rice. A continuous wave technique for the measurement of the elastic properties of cortical bone. *Journal of Biomechanics*. 17:349-361, 1984.
- [12] Peng L, Bai J, Zeng X, ZhouY. Comparison of isotropic and orthotropic material property assignments on femoral finite element models under two loading conditions. *Medical Engineering and Physics*; 28:227-233, 2006.
- [13] Baca V, Horak Z, Mikulenka P, Dzupa V. Comparison of an inhomogeneous orthotropic and isotropic material models used for FE analyses. *Medical Engineering and Physics*, 2008.
- [14] W. A. Kalender. A phantom for standardization and quality control in spinal bone mineral measurements by qct and dxa: design considerations and specifications. *Medical Physics*, 19:583-586, 1992.
- [15] Taylor WR, Roland E, Ploeg H, Hertig D, Klabunde R, Warner MD. Determination of orthotropic bone elastic constants using FEA and modal analysis. *Journal of Biomechanics*, 35:767-773, 2002.
- [16] Wirtz DCH, Pandorf T, Portheime F, Radermache K, Schifflers N. Concept and development of an orthotropic FE model of the proximal femur. *Journal of Biomechanics*, 36:289-293, 2003.
- [17] Bergmann G, Deuretzbacher G, Heller M, Graichen F, Rohlmann A, Strauss J, Duda, G.N. Hip contact forces and gait patterns from routine activities. *Journal of Biomechanics*, 34:859-871, 2001.